



**Optimising the
FAMOUS climate
model: inclusion of
global carbon cycling**

J. H. T. Williams et al.

Optimising the FAMOUS climate model: inclusion of global carbon cycling

J. H. T. Williams¹, R. S. Smith², P. J. Valdes¹, B. B. B. Booth³, and A. Osprey²

¹BRIDGE, School of Geographical Sciences, University of Bristol, Bristol, BS8 1SS, UK

²Department of Meteorology, University of Reading, Reading, RG6 6BB, UK

³Met Office Hadley Centre, FitzRoy Road, Exeter, EX1 3PB, UK

Received: 24 August 2012 – Accepted: 21 September 2012 – Published: 4 October 2012

Correspondence to: J. H. T. Williams (jonny.williams@bristol.ac.uk)

Published by Copernicus Publications on behalf of the European Geosciences Union.

[Title Page](#)

[Abstract](#)

[Introduction](#)

[Conclusions](#)

[References](#)

[Tables](#)

[Figures](#)



[Back](#)

[Close](#)

[Full Screen / Esc](#)

[Printer-friendly Version](#)

[Interactive Discussion](#)

Abstract

FAMOUS fills an important role in the hierarchy of climate models, both explicitly resolving atmospheric and oceanic dynamics yet being sufficiently computationally efficient that either very long simulations or large ensembles are possible. An improved set of carbon cycle parameters for this model has been found using a perturbed physics ensemble technique. This is an important step towards building the “Earth System” modelling capability of FAMOUS, which is a reduced resolution, and hence faster running, version of the Hadley Centre Climate model, HadCM3. Two separate 100 member perturbed parameter ensembles were performed; one for the land surface and one for the ocean. The land surface scheme was tested against present day and past representations of vegetation and the ocean ensemble was tested against observations of nitrate. An advantage of using a relatively fast climate model is that a large number of simulations can be run and hence the model parameter space (a large source of climate model uncertainty) can be more thoroughly sampled. This has the associated benefit of being able to assess the sensitivity of model results to changes in each parameter. The climatologies of surface and tropospheric air temperature and precipitation are improved relative to previous versions of FAMOUS. The improved representation of upper atmosphere temperatures is driven by improved ozone concentrations near the tropopause and better upper level winds.

1 Model description and motivation

The climate model used in this work is FAMOUS (Jones et al., 2005; Smith et al., 2008), which is a lower resolution version of the HadCM3 climate model (Pope et al., 2000; Gordon et al., 2000). The atmospheric component of FAMOUS has a resolution of $5^{\circ} \times 7.5^{\circ}$ (compared to the $2.5^{\circ} \times 3.75^{\circ}$ of HadCM3) and has 11 vertical levels, a significant reduction compared to the 19 in HadCM3. The ocean has twice the resolution of the atmosphere (i.e. $2.5^{\circ} \times 3.75^{\circ}$) and 20 vertical levels. HadCM3’s ocean resolution is

GMDD

5, 3089–3129, 2012

Optimising the FAMOUS climate model: inclusion of global carbon cycling

J. H. T. Williams et al.

[Title Page](#)

[Abstract](#)

[Introduction](#)

[Conclusions](#)

[References](#)

[Tables](#)

[Figures](#)



[Back](#)

[Close](#)

[Full Screen / Esc](#)

[Printer-friendly Version](#)

[Interactive Discussion](#)



of MOSES2.2 in FAMOUS. It is possible to run MOSES 2.2 using static or dynamic vegetation, the latter using the TRIFFID dynamic vegetation model (Cox, 2001). Future research with this configuration of FAMOUS will, in part, aim to examine climates of the past where human intervention in the structure of the land surface was negligible or zero. Therefore, the urban fraction is set to zero throughout this work.

In addition to land surface processes, the ocean carbon cycle is also simulated within the model. This sub-model is known as HadOCC, the Hadley Centre Ocean Carbon Cycle model (Palmer and Totterdell, 2001). HadOCC is an “ecosystem model” due to its explicit inclusion of phytoplankton and zooplankton populations. These populations are limited purely by nitrate availability (that is, nitrate is the only nutrient simulated) and in addition to plankton, total CO₂, alkalinity and detrital material densities are calculated. The flux of carbon through the NPZD (nutrient-phytoplankton-zooplankton-detritus) model is coupled to the prognostic flux of nitrogen through constant C:N, “Redfield”, ratios (Palmer and Totterdell, 2001; Redfield, 1958).

Climate models contain many adjustable parameters, each with an associated uncertainty. This uncertainty comes, for some parameters, from the inability to measure the value of an observable to arbitrary accuracy. For example N_{L0} – the ratio of nitrogen to carbon in a leaf, a model constant representative of a given plant functional type (e.g. shrubs) – is a measurable quantity at the plant leaf scale. The uncertainty associated with this parameter comes from upscaling site measurements to a global quantity. There is also some uncertainty from structural parameters in model parameterisations, which do not have a directly observable equivalent in the real world. For example, LAI_{min} is a competition parameter which controls how plants will expand. This is not a directly observable quantity, instead the plausible uncertainty ranges are established largely from insight from the model developers based on how variations in this parameter influence properties of the simulations that are observable, such as forest extent. Previous versions of FAMOUS have had their parameters tuned through different procedures (Jones et al., 2005; Smith et al., 2008; Gregoire et al., 2010), but the combination of a complex land surface scheme coupled to dynamic vegetation

Optimising the FAMOUS climate model: inclusion of global carbon cycling

J. H. T. Williams et al.

[Title Page](#)[Abstract](#)[Introduction](#)[Conclusions](#)[References](#)[Tables](#)[Figures](#)[Back](#)[Close](#)[Full Screen / Esc](#)[Printer-friendly Version](#)[Interactive Discussion](#)

Optimising the FAMOUS climate model: inclusion of global carbon cycling

J. H. T. Williams et al.

[Title Page](#)

[Abstract](#)

[Introduction](#)

[Conclusions](#)

[References](#)

[Tables](#)

[Figures](#)



[Back](#)

[Close](#)

[Full Screen / Esc](#)

[Printer-friendly Version](#)

[Interactive Discussion](#)

and an ocean carbon cycle has not been used before in FAMOUS. The computational efficiency of FAMOUS provides an opportunity to explore relationships between parameters and model response and hence identify the set of structural parameters in this new model which give the highest fidelity output when compared to appropriate observations. To this end, building on the tuning of atmosphere and ocean parameters by Gregoire et al. (2010), two 100 member perturbed physics ensembles were performed; one for the land surface and one for the ocean carbon cycle variables. The full coupling of the terrestrial and ocean carbon cycles is ongoing and will be described in a forthcoming paper.

For both the land surface and the ocean perturbed physics ensembles, the set up of the control run was the same. Constant, preindustrial levels of CO₂ in the atmosphere (290 ppmv) were used. For the vegetation distribution, the control and all ensemble members were initialised at 1860 values and each ensemble member was run for 200 yr; this was found to be more than sufficient for equilibrium to be reached. For all simulations using dynamic vegetation in this study, the “equilibrium” mode was used, which enables more rapid convergence of the final distribution of PFTs under constant forcing conditions. This works by coupling TRIFFID to MOSES only every 5 yr (although this time period can be altered if desired) and thereby exchanging the carbon flux output during that time with the vegetation scheme. After each iteration of this coupling, TRIFFID is then run using a large timestep of 100 yr. This enables equilibrated states of even the slowest responding variables to be approached more rapidly. More information on the technical details of this coupling can be found in Cox (2001). For the ocean ensemble, a run length of 200 yr was also found to be sufficient for the variables of interest to equilibrate, even when the ocean tracers were initialised with constant values throughout the ocean. It should be noted that there is no equivalent “equilibrium” mode for the ocean carbon cycle as is used for the land surface. To bring the deep ocean into thermal and carbon equilibrium with the surface would take several thousand years and so it is unfeasible to run a 100 member ensemble where each member is run for this long. The ocean ensemble is validated using near-surface observations (5 m depth)

where equilibrium is easily reached in 200 yr. Climatologies were constructed for the last 30 yr of each ensemble member.

2 Perturbed parameters – land surface

The number of structural parameters present in this version of FAMOUS is large and since the main departure from previous versions concerns the carbon cycle (both on land and in the ocean) it was deemed appropriate to find an optimum set of parameters which best reflect the present day status of the biosphere.

Previous work (Booth et al., 2012) used the Latin hypercube method (e.g. Gregoire et al., 2010) to efficiently sample parameter space within bounds reflecting the uncertainty with which these model parameters are known. Booth et al. were then able to demonstrate that uncertainties in the values of carbon cycle parameters can give rise to significant uncertainty in projections of future climate. The present study also uses the Latin hypercube method to vary the same parameters as Booth et al. (with the addition of R_{grow}) which are described in Table 1. Note that the values for all the plant functional types (PFTs) are co-varied, i.e., if the value of certain parameter for broadleaf trees is doubled, the equivalent parameters for the 4 other PFTs will also be doubled, as in Booth et al. (2012).

The parameters in Table 1 are now described in detail.

- N_{L0} – The “top leaf nitrogen concentration”. This is defined as the amount of nitrogen per amount of carbon and has the units kg N/kg C (Cox et al., 1999).
- f_0 – The ratio of CO_2 concentrations inside and outside leaves at zero humidity deficit (Cox et al., 1999).
- LAI_{min} – Any PFT must achieve this value of the Leaf Area Index before it starts to contend with other PFTs for growing area (Cox, 2001).

Optimising the FAMOUS climate model: inclusion of global carbon cycling

J. H. T. Williams et al.

Title Page

Abstract

Introduction

Conclusions

References

Tables

Figures



Back

Close

Full Screen / Esc

Printer-friendly Version

Interactive Discussion



- Q_{10} – This parameter describes the how the respiration rate of soil varies with temperature. This is done using a power law multiplier, the exponent of which rises by 1.0 when the temperature rises by 10°C (Cox et al., 1999).
 - The “KAPS” parameter, which describes the specific rate of soil respiration at 25°C and at optimal soil moisture, is co-varied with Q_{10} to maintain respiration at this temperature at the standard model rate.
- $V_{\text{crit},\alpha}$ – This is a new parameter which has been integrated into the model code and is defined by $V_{\text{crit}} = V_{\text{wilt}} + V_{\text{crit},\alpha} (V_{\text{sat}} - V_{\text{wilt}})$ where, V_{crit} , V_{sat} and V_{wilt} are “by volume” soil moisture concentrations (m^3 of water per m^3 of soil). Below V_{wilt} , leaf stomata close; V_{sat} is the soil moisture amount at the point of saturation and V_{crit} is the amount above which PFTs are not water limited. The fact that $V_{\text{crit},\alpha}$ varies between zero and one means that V_{crit} varies between V_{wilt} and V_{sat} (Cox et al., 1999).
- T_{upp} – This is one of two parameters which affect how photosynthesis varies with temperature (Cox et al., 2000), the other being T_{low} . As can be seen from Table 1, there is actually only one free parameter for T_{upp} , because the values for NT, C3, C4 and shrubs are also covaried. In addition, the values of T_{low} are as follows; $T_{\text{low,BT}} = T_{\text{upp,BT}} - 36$, $T_{\text{low,NT}} = T_{\text{upp,BT}} - 41$, $T_{\text{low,C3}} = T_{\text{upp,BT}} - 36$, $T_{\text{low,C4}} = T_{\text{upp,BT}} - 23$, $T_{\text{low,shrub}} = T_{\text{upp,BT}} - 36$.
 - Booth et al. (2012) present a variable transformation and define $T_{\text{opt}} = T_{\text{upp}} - 4.0$ here. This is because T_{opt} is more directly observable. The full definitions of T_{upp} and T_{low} are retained here for completeness and to aid the understanding of the model user.
- R_{grow} – The “growth respiration fraction”. The total respiration, R_{p} , of plants can be divided into those amounts required for the maintenance, R_{pm} , and growth, R_{pg} , of the plant, where R_{pg} is defined as $R_{\text{pg}} = R_{\text{grow}} (\Pi_{\text{G}} - R_{\text{pm}})$, and Π_{G} is the “gross

Optimising the FAMOUS climate model: inclusion of global carbon cycling

J. H. T. Williams et al.

Title Page

Abstract

Introduction

Conclusions

References

Tables

Figures

⏪

⏩

◀

▶

Back

Close

Full Screen / Esc

Printer-friendly Version

Interactive Discussion



canopy photosynthesis” (Cox et al., 1999). A corollary of this set of definitions is that R_{pg} is also equal to one third of the net primary productivity, $\Pi = \Pi_G - R_p$. More information on the precise definition of these parameters can be found in Cox et al. (1999).

5 Previous work by Gregoire et al. also used an ensemble approach to identify optimal configurations of FAMOUS with respect to atmosphere and ocean parameters which are known to have a significant effect on the climatology (Gregoire et al., 2010; Jones et al., 2005; Murphy et al., 2004). It was therefore desirable that the results of this earlier work were incorporated into the present optimisation framework and, to this
10 end, the ten highest scoring models from Gregoire et al. were sampled using a further “state parameter”, β . The incorporation of this extra parameter means that it is not just the carbon cycle’s uncertainties which are being perturbed in the ensemble but also those of the physical atmosphere and ocean which have previously been shown have a significant impact on model climate (Jones et al., 2005). The fact that only the 10
15 highest scoring models from Gregoire et al. are chosen for examination here means that it is only the more plausible combinations of values of the physical parameters which are sampled.

The state parameter, β , was varied continuously between 0 and 1 using the same Latin hypercube sampling technique as for all the other model parameters. However,
20 β was then converted to an integer value between one and ten which was used to discriminate between the ten highest scoring sets of parameters from Gregoire et al. Therefore, in total, eight free parameters were varied and an ensemble of one hundred members was run. For Latin hypercube sampling, it is advantageous to have at least
25 ten times as many ensemble members as free parameters; this condition is therefore easily fulfilled in this case. It would have been statistically advantageous to vary each parameter independently for each PFT but this would have increased the necessary size of the ensemble beyond that which was possible due to computational constraints.

Optimising the FAMOUS climate model: inclusion of global carbon cycling

J. H. T. Williams et al.

[Title Page](#)[Abstract](#)[Introduction](#)[Conclusions](#)[References](#)[Tables](#)[Figures](#)[⏪](#)[⏩](#)[◀](#)[▶](#)[Back](#)[Close](#)[Full Screen / Esc](#)[Printer-friendly Version](#)[Interactive Discussion](#)

3 Perturbed parameters – ocean

A further ensemble, perturbing the parameters in the HadOCC sub-model was also carried out. Table 2 shows the control values of the twenty structural parameters in the ocean carbon cycle of FAMOUS which are varied in this work. These parameters are described in Table 2 of Palmer and Totterdell (2001).

All parameters in Table 2 were varied by $\pm 50\%$ in the Latin hypercube-generated ensemble (as recommended by the code developers of HadOCC) and, as with the land surface, an ensemble of 100 members was run. Since there are twenty structural parameters listed in Table 2, to vary each parameter individually would require at least two hundred simulations to be performed which is currently impractical. Therefore, the parameters were subdivided into five categories by their compartmentalisation in the model (the “free parameter index” in Table 2): (1) C:N ratio (2) phytoplankton-specific parameters (3) zooplankton-specific parameters (4) detritus-specific parameters (5) carbonate precipitation. Each parameter represented by these five indices was co-varied and therefore the condition of having at least ten times as many ensemble members as free model parameters (i.e. 5) is met. This method of co-variation was decided upon after discussions with the HadOCC code developers (Paul Halloran of the Met Office Hadley Centre, personal communication, 2011) and is in line with the work of Booth et al. (2012) whose co-variation scheme is used here for the land surface parameter perturbations.

Due to the inclusion of the state parameter, β , in the land carbon cycle simulations, some ocean parameters differ between the best land surface and ocean simulations. It has been shown however that these differences to the ocean diffusivity and viscosity (Gregoire et al., 2010) make no significant difference to the model climatology.

Optimising the FAMOUS climate model: inclusion of global carbon cycling

J. H. T. Williams et al.

[Title Page](#)

[Abstract](#)

[Introduction](#)

[Conclusions](#)

[References](#)

[Tables](#)

[Figures](#)



[Back](#)

[Close](#)

[Full Screen / Esc](#)

[Printer-friendly Version](#)

[Interactive Discussion](#)



4 How the perturbed physics ensembles were evaluated

4.1 Land surface

4.1.1 The Amazon now

Evaluation of how well the land surface ensemble members matched observations was done by comparison with data adapted from the Advanced Very High Resolution Radiometer (AVHRR), forming part of the International Geosphere – Biosphere Programme (Loveland et al., 2000). Figure 1 shows which of the surface types used in TRIFFID has the highest fraction within each grid box and additionally what the fractional coverage of the dominant tile fraction in each gridbox is equal to.

From Fig. 1 it is clear that there are large areas of the world where the dominant tile fraction is significantly different from 1. The global average of the quantity given in the right-hand side of Fig. 1 is 0.63 and the spatial standard deviation is 0.18. The equivalent value for the ensemble mean is 0.72 with a spatial standard deviation of 0.12. The combination of these values (higher mean, lower variability) show that the simulations tend to favour non-coexisting PFTs in each gridbox, compared to observations. For this reason, the dominant PFT in a gridbox is used to evaluate the efficacy of the different ensemble members' reproduction of vegetation cover. Figure 1 shows that the Amazon region is a good one to concentrate on because it is a large area where the fraction of the dominant surface type is close to 1 and also because of the region's known effects on global climate (e.g. Werth and Avissar, 2002).

The Amazon region is defined to be 40°W–80°W, –20°S–10°N in this work and is predominantly defined by its BT coverage (Fig. 1). In this region there are 28 land gridboxes and in the observations 22 are BT, 4 are C4, 1 is bare soil and 1 is shrub. Figure 2 shows a histogram of the fractional agreement between PFTs in the ensemble and the observations, that is, how many of the 28 grid boxes are assigned the same PFT in the ensemble members and in observations. In this instance the term “PFTs” is broadened to include bare soil cover.

Optimising the FAMOUS climate model: inclusion of global carbon cycling

J. H. T. Williams et al.

[Title Page](#)

[Abstract](#)

[Introduction](#)

[Conclusions](#)

[References](#)

[Tables](#)

[Figures](#)



[Back](#)

[Close](#)

[Full Screen / Esc](#)

[Printer-friendly Version](#)

[Interactive Discussion](#)



parameter values plotted on the vertical axis are normalised between 0 and 1, where 0 represents the lowest value of the parameter chosen by the Latin hypercube sampling, and 1 represents the highest, with all other values being linearly interpolated between the two.

Figure 3 shows that some of the credible parameter ranges obtained from the ensemble are considerably smaller than others. For example, T_{upp} could take essentially any value sampled in the ensemble, whereas f_0 is found to be limited to higher values and $V_{\text{crit},\alpha}$ to lower values. Numerically, the parameters are fractionally constrained as follows: f_0 (31 %), LAI_{min} (88 %), N_{L0} (53 %), R_{grow} (62 %), T_{upp} (92 %), Q_{10} (78 %), $V_{\text{crit},\alpha}$ (30 %) and β (59 %). The fact that the largest parameter uncertainty lies with T_{upp} poses a challenge for future carbon cycle changes, where temperature dependences of plant photosynthesis (represented by this parameter) is the dominant uncertainty in future responses (Booth et al., 2012). This result suggests that contemporary plant distributions do not provide a potential constraint on the range of plausible T_{upp} values, and hence a way to constrain the range of future changes. This analysis, however, does illustrate that model comparisons with observed vegetation cover may provide a stronger constraint on other parameters (F_0 , N_{L0} and $V_{\text{crit},\alpha}$), that have important rôles in the hydrological response.

4.1.3 The Amazon in the past

The Amazon rainforest has been part of the landscape of South America for millions of years. However, its structure has not remained constant throughout that time (Maslin et al., 2005). Since the reproduction of the structure of the Amazon is highly sensitive to model parameters (see Fig. 2 for example), it is important to further validate the model by perturbing the simulations in another way. This is done by changing the orbital forcing of the $\alpha 7$ simulations. It is known that the forest's structure was similar to today during the Mid-Holocene (6000 yr ago) and so the $\alpha 7$ simulations were run for an orbital configuration corresponding to 6000 yr ago and compared to the equivalent for the present day. The leaf area index (LAI) is a parameterisation of the area of leaf cover per

Optimising the FAMOUS climate model: inclusion of global carbon cycling

J. H. T. Williams et al.

[Title Page](#)

[Abstract](#)

[Introduction](#)

[Conclusions](#)

[References](#)

[Tables](#)

[Figures](#)

[⏪](#)

[⏩](#)

[◀](#)

[▶](#)

[Back](#)

[Close](#)

[Full Screen / Esc](#)

[Printer-friendly Version](#)

[Interactive Discussion](#)



unit area of ground (Law et al., 2008) and the differences between the mid-Holocene (and LGM) and their $\alpha 7$ equivalents are shown in Fig. 4.

It is clear from Fig. 4 that the LAI is generally increased across the Amazon for all of the mid-Holocene simulations with the exception of that shown in Fig. 4a. Maslin et al. have also shown that at the Last Glacial Maximum (LGM) 21 000 yr ago, the density of the Amazon was reduced, as represented by a reduction in LAI. Only Fig. 4h shows a considerable reduction in LAI at the LGM, as required for agreement with the work of Maslin et al. and this is in agreement with the result in Fig. 4a which also identifies this simulation as containing a suitable set of parameters. Therefore a combination of present day observations and paleoclimatic reconstructions of the Amazon rainforest has been used to identify a realistic set of terrestrial carbon cycle parameters suitable for use in further research.

Figure 5 shows the dominant PFT in each gridbox and its fractional coverage for the best performing ensemble member identified in the preceding discussion; it is analogous to Fig. 1 which shows the equivalent data for the observations.

The biases common to the $\alpha 7$ ensemble members (discussed at the end of Sect. 4.1.1) are clearly seen in Fig. 5, as is the tendency for TRIFFID to not have different PFTS cohabiting in the same gridbox. It should be emphasised that some of these biases may be associated with issues within MOSES/TRIFFID but other biases may be associated with problems with the control climate. For instance, FAMOUS has a tendency to make Australia too wet and hence the Australian desert area is underestimated. Unfortunately, TRIFFID cannot be run offline and hence it is not possible to explicitly separate the climate biases from TRIFFID biases.

4.2 Ocean

The fidelity of the ocean carbon cycle is considered by comparing the concentration of the rate-limiting nutrient in the system, nitrate, with global observations from the World Ocean Atlas (Garcia et al., 2006). The annual mean concentration at 5 m depth in the simulations is compared with the average of the surface and 10 m depth values from

Optimising the FAMOUS climate model: inclusion of global carbon cycling

J. H. T. Williams et al.

[Title Page](#)

[Abstract](#)

[Introduction](#)

[Conclusions](#)

[References](#)

[Tables](#)

[Figures](#)



[Back](#)

[Close](#)

[Full Screen / Esc](#)

[Printer-friendly Version](#)

[Interactive Discussion](#)



Optimising the FAMOUS climate model: inclusion of global carbon cycling

J. H. T. Williams et al.

[Title Page](#)

[Abstract](#)

[Introduction](#)

[Conclusions](#)

[References](#)

[Tables](#)

[Figures](#)

[⏪](#)

[⏩](#)

[◀](#)

[▶](#)

[Back](#)

[Close](#)

[Full Screen / Esc](#)

[Printer-friendly Version](#)

[Interactive Discussion](#)

the observations. The quality of the model fit to the data is calculated using the Arcsine Mielke skill (AMS) score which gives a score of 1 for perfect correlation and -1 for perfect anti-correlation. If a model field bears no resemblance to the observations then the score will be zero. Further information regarding the AMS can be found in Jones et al. (2005) and Watterson (1996), for example. The nitrate data in the World Ocean Atlas data is given on 1° resolution and therefore it must be regridded onto the model grid of $2.5^\circ \times 3.75^\circ$ before meaningful comparisons can be made.

Of the 100 ensemble members, 4 gave unphysical values for the nitrate concentration in the climatologies; Fig. 6 shows the remaining 96 members' AMS values.

It is important that when a model parameter is varied to find an optimum configuration, the range of values of that parameter give rise to a broad range of model responses. It is apparent from Fig. 6 that this condition is met for nitrate, where the AMS ranges from 0.040 to 0.72 (mean 0.51) with a standard deviation of 0.16. On the contrary, if one compares the sea surface temperature from the model ensemble with observations from Rayner et al. (2003), the standard deviation is just 0.0017 around a mean of 0.85.

It should be noted here that, in reality, the productivity of the Southern Ocean is iron limited (Boyd et al., 2000). Therefore, as a further check of the validity of this method, the same AMS calculations were performed but excluding ocean points south of 60° S. Even with this restriction on the area of study, the parameter set identified as the best in Fig. 6 still provides an AMS score of 0.67, compared to a maximum of 0.72 and a minimum of 0.05. The average difference between the AMS scores for the global and no-Southern-Ocean cases is $+0.02$ and the standard deviation of this quantity is 0.04. Therefore the $+0.05$ difference between the value of 0.72 for the global case and 0.67 for the no-Southern-Ocean case is within this range of variability. It is reassuring that, even excluding the Southern Ocean from the data analysis, the parameters found to give the best global nitrate concentration still give a high fidelity reproduction compared to the majority of the other ensemble members.

Optimising the FAMOUS climate model: inclusion of global carbon cycling

J. H. T. Williams et al.

[Title Page](#)

[Abstract](#)

[Introduction](#)

[Conclusions](#)

[References](#)

[Tables](#)

[Figures](#)



[Back](#)

[Close](#)

[Full Screen / Esc](#)

[Printer-friendly Version](#)

[Interactive Discussion](#)



The parameters from the highest scoring member of the ensemble (as identified in Fig. 6) are given in Table 3 along with their relationship to the control value. It is encouraging that all but one of the 5 free model parameters deviate noticeably from the control value as it adds weight to the necessity of the exercise. Additionally, none of the 5 parameters are at the extremes of the distribution of parameter space ($\pm 50\%$) when compared to the control simulation, which shows that the postulated range of parameters is plausible.

Scott et al. (2011) have performed a similar perturbed physics ensemble of HadOCC runs to that carried out here and although they use a considerably larger parameter set than the present authors (1000 set of parameters), the simulations are run in 1 dimension and for run lengths of just 9 yr to examine the model's internal sensitivity to model parameters, without calling for model-data comparison as performed here. In addition, Doney et al. (2004) have shown that the background physical state (e.g. the ocean circulation) is perhaps more important for the realism of the ocean carbon cycle than the model parameters themselves. These studies, along with the comparison to observed ocean nitrate concentration performed here, clearly show that a more coordinated study of ocean carbon cycle parameter uncertainties is required and that the work presented here is a step towards achieving the goal of better constrained parameters affecting the global carbon budget.

Now that plausible parameters have been identified for the land and ocean carbon cycles, it is necessary to examine the climatology of this new version of FAMOUS to ensure that the results obtained do indeed represent an improvement in model skill.

5 Climatology and validation

Since the first FAMOUS documentation paper (Jones et al., 2005), there have been a number of improvements made. Smith et al. (2008) described advances in the representation of sea ice and ozone as well as the introduction of the HadOCC ocean carbon cycle component. Smith (2012) shows improved upper level winds through the

introduction of a Rayleigh friction term at the top of the atmosphere and also described other changes relating to, for example, ocean-solar radiation interactions and the effect of snow at coastal points due to the fractional land-sea mask in FAMOUS (e.g. Smith et al., 2008). The climatologies of runs using the newly identified carbon cycle parameter sets are now described.

5.1 Atmosphere and land surface

5.1.1 Near-surface air temperature

It is important to confirm that the new versions of FAMOUS described here are compatible with those published previously (Jones et al., 2005; Smith et al., 2008; Smith, 2012) and with HadCM3. This is because FAMOUS was originally calibrated against HadCM3 in order to provide an analogous climatology but with significantly reduced run times. The FAMOUS simulations in question (denoted by their unique 5 letter Met Office Unified Model simulation index) are given below and are denoted a generation number to indicate the order of their documentation date. The version of the land surface scheme, MOSES, is also given.

- ADTAN (Jones et al., 2005) – MOSES 1
 - Generation 1
- XDBUA (Smith et al., 2008) – MOSES 1
 - Generation 2
- XFHCC (Smith, 2012) – MOSES 1
 - Generation 3
- XFHCU (optimised carbon cycle parameters) – MOSES 2.2 (fixed vegetation)
 - Generation 4a

Optimising the FAMOUS climate model: inclusion of global carbon cycling

J. H. T. Williams et al.

[Title Page](#)

[Abstract](#)

[Introduction](#)

[Conclusions](#)

[References](#)

[Tables](#)

[Figures](#)



[Back](#)

[Close](#)

[Full Screen / Esc](#)

[Printer-friendly Version](#)

[Interactive Discussion](#)



- XFHCS (optimised carbon cycle parameters) – MOSES 2.2 + TRIFFID (dynamic vegetation)
 - Generation 4b

The generation 3 simulation, XFHCC, is the most recently documented version of FAMOUS prior to this work although most work currently being undertaken with FAMOUS uses XDBUA (the generation 2 model) or XFXWB (Smith, 2012). The only major structural difference between XFXWB and XFHCC (the generation 3 model used here) is the inclusion of Rayleigh Friction in the upper 3 atmospheric model levels; a change which has been shown to improve the climatology. XFHCC is therefore chosen above XFXWB as the generation 3 model to enhance traceability in the documentation of FAMOUS; noteworthy differences between XFXWB and XFHCC are described in Smith (2012).

All previously documented versions of FAMOUS have used the MOSES 1 land surface scheme and a fixed vegetation distribution and so the newly optimised description of the model represents a step change in model complexity. Figure 7 shows the 1.5 m air temperature for the simulations described above and Table 4 shows the corresponding AMS values.

One particularly apparent aspect of the FAMOUS results shown in Fig. 7 is the persistent cold bias in the Northern Hemisphere in DJF although this is significantly improved in more recent versions of the model compared to the 1st generation. Generations 3, 4a and 4b are strikingly similar in DJF with a cold bias which is shifted east compared to generation 2. In addition, the agreement between FAMOUS and HadCM3 is noticeably better in JJA compared to DJF; this is evident in all versions of the model.

Another result (not shown) is that the introduction of MOSES 2.2 (with fixed vegetation cover) whilst maintaining the un-optimised carbon cycle parameters overcompensates for the Northern Hemisphere winter cold bias and introduces a summer warm bias. Using the optimised parameter set does leave some cold bias in place (Fig. 7) but significantly improves this “new” summer warm bias. So in summary, the introduction

Optimising the FAMOUS climate model: inclusion of global carbon cycling

J. H. T. Williams et al.

[Title Page](#)

[Abstract](#)

[Introduction](#)

[Conclusions](#)

[References](#)

[Tables](#)

[Figures](#)



[Back](#)

[Close](#)

[Full Screen / Esc](#)

[Printer-friendly Version](#)

[Interactive Discussion](#)



of MOSES 2.2 provides an annual mean temperature climatology which is as good as any of the previously documented versions of FAMOUS. If the vegetation is fixed to observations of the contemporary biosphere, the optimisation procedure described above provides not only a good global AMS score, but also helps to alleviate the persistent DJF Northern Hemisphere cold bias.

5.1.2 Vertical temperature profile

Having studied the ability of FAMOUS to reproduce HadCM3's surface temperature distribution, the air temperature aloft is now examined with respect to the ECMWF 40 yr reanalysis (Uppala et al., 2005). The vertical temperature structure of FAMOUS was last studied in Smith et al., 2008 (Fig. 5) and Fig. 8 shows an updated version of this figure but with simulation output plotted with respect to ERA-40 data rather than ERA-15.

The atmospheric resolution of FAMOUS is significantly reduced compared to HadCM3 (11 vertical levels compared to 19); indeed there is frequently just a single model layer at pressures lower than the tropopause (Smith et al., 2008). Therefore, the ability of the generation 4b version of FAMOUS to accurately reproduce the temperature structure of HadCM3 and ERA-40 up to 10 mbar (the lowest value pressure level available for all the simulations presented here) is very encouraging.

One reason for the improvement in upper-atmosphere temperature profiles (along with improved upper level winds as described in Smith, 2012) is due to the different ozone parameterisations in the separate model versions and these values are shown in Table 5.

5.1.3 Precipitation

Smith et al. (2008) used the CPC Merged Analysis of Precipitation (CMAP) dataset (Xie and Arkin, 1997) to validate the 2nd generation FAMOUS model, XDBUA, and this dataset is also used here. Figure 9 shows the annual mean total precipitation for the

Optimising the FAMOUS climate model: inclusion of global carbon cycling

J. H. T. Williams et al.

[Title Page](#)

[Abstract](#)

[Introduction](#)

[Conclusions](#)

[References](#)

[Tables](#)

[Figures](#)



[Back](#)

[Close](#)

[Full Screen / Esc](#)

[Printer-friendly Version](#)

[Interactive Discussion](#)



CMAP climatology, the 3rd generation model, XFHCC and the 4th generation models XFHCU (fixed vegetation) and XFHCS (dynamic vegetation). This figure also shows the respective AMS values.

The land surface scheme of a climate model can be expected to have a significant effect on precipitation over land. For example, a significant difference between the land surface schemes of the 4th generation versions of FAMOUS and those documented previously is the introduction of plant functional types which can individually affect the fluxes of water and CO₂ at the land-atmosphere interface.

In light of this, it is reassuring that in both 4th generation versions of FAMOUS the global representation of precipitation is improved compared to the 3rd generation version as shown by the AMS scores in the subtitles to Fig. 9b–d. The main features to note are the improvement to the (positive and negative) biases over the equatorial Pacific in Fig. 9c, d and also over the Amazon basin in Fig. 10c, where the vegetation is held constant. There is a small increase in the positive bias in the equatorial Atlantic in the 4th generation models but overall the global precipitation is noticeably improved with respect to the earlier version.

Figure 9a clearly shows that the areas of highest rainfall are located in the ITCZ and SPCZ (Inter-Tropical and South Pacific Convergence Zones). What this means is that the precipitation anomalies with respect to the CMAP observations in Fig. 9b–d mainly highlight these areas. Figure 10 shows the same data as Fig. 9 but only for the northern and southern mid-latitudes (30°–60°) and Table 6 gives the respective AMS scores.

From Figs. 9 and 10 as well as Table 6 it can be seen that although the global, tropical and southern mid-latitude AMS is improved in the generation 4 simulations compared to the generation 3 version, this is not the case for northern mid-latitudes. This slight deterioration is due to an increase in the positive bias over Western North America and an increase in the negative bias over the Northern Pacific.

Optimising the FAMOUS climate model: inclusion of global carbon cycling

J. H. T. Williams et al.

[Title Page](#)

[Abstract](#)

[Introduction](#)

[Conclusions](#)

[References](#)

[Tables](#)

[Figures](#)



[Back](#)

[Close](#)

[Full Screen / Esc](#)

[Printer-friendly Version](#)

[Interactive Discussion](#)



5.2 Ocean nitrate

Figure 11 shows the annual average nitrate concentration for observations from the World Ocean Atlas (Garcia et al., 2006) and for the generation 3 and 4a simulations.

There are no significant differences between the nitrate distributions for the two generation 4 models XFHCU – Fig. 11c – and XFHCS (not shown) which is expected because these simulations differ only in their representation of terrestrial vegetation. When comparing Fig. 11b and c however, a marked improvement in FAMOUS' ability to reproduce the observed nitrate concentration is seen between generation 3 and 4, which is clearly manifested in a significant increase in the AMS score for XFHCU as shown above Fig. 11b, c. Clearly this is the expected result because the optimised ocean carbon cycle parameters used in XFHCU were tuned to the nitrate concentration in Fig. 11a. However this does provide a good illustration of the power of the tuning method employed in this work. For example, the large positive bias in the equatorial Pacific is significantly reduced and, although the positive bias in the south Atlantic is increased, the overall Southern Ocean bias is markedly reduced. As previously mentioned however, the Southern Ocean bias is of lesser importance here since the ocean productivity in this region is, in reality, iron limited (Boyd et al., 2000).

6 Conclusions and future work

The two new versions of FAMOUS presented here represent an important increase in model complexity compared to previous versions of the model, with the inclusion of surface tiling into 9 sub-types and the flexibility to include dynamic vegetation response to climate forcings. The carbon cycle parameters of both the land surface and the ocean have been tuned to observations and reanalysis data and the climatologies of the new versions of the model have been shown to be noticeably improved.

Concerning the terrestrial carbon cycle, the use of a large ensemble of 100 climate simulations has enabled the determination of sensible ranges of the parameters varied

Optimising the FAMOUS climate model: inclusion of global carbon cycling

J. H. T. Williams et al.

[Title Page](#)

[Abstract](#)

[Introduction](#)

[Conclusions](#)

[References](#)

[Tables](#)

[Figures](#)



[Back](#)

[Close](#)

[Full Screen / Esc](#)

[Printer-friendly Version](#)

[Interactive Discussion](#)



Optimising the FAMOUS climate model: inclusion of global carbon cycling

J. H. T. Williams et al.

[Title Page](#)

[Abstract](#)

[Introduction](#)

[Conclusions](#)

[References](#)

[Tables](#)

[Figures](#)

[⏪](#)

[⏩](#)

[◀](#)

[▶](#)

[Back](#)

[Close](#)

[Full Screen / Esc](#)

[Printer-friendly Version](#)

[Interactive Discussion](#)



in the ensemble methodology. It is clear that certain parameters are significantly better constrained than others by this work. For example, the 7 ensemble members which are seen to give the best representation of the Amazon rainforest only account for 30 % of the variation of the parameter controlling the critical soil moisture ($V_{\text{crit},\alpha}$) whereas the same 7 simulations encompass 92 % of the parameter range of the T_{upp} parameter which, in part, controls the response of photosynthesis with temperature. This last result concerning T_{upp} suggests that comparisons with land surface coverage do not provide a constraint on the future land carbon cycle uncertainty identified here and in Booth et al. (2012). It does raise the interesting implication, however, that comparisons of land surface coverage between observations and simulations may constrain other land carbon cycle parameters more closely tied to the hydrological response within the model.

Despite including many elements of the carbon cycle, the work presented here fixes the atmospheric concentration of CO_2 at preindustrial levels. This clearly limits the degree to which the newly modelled carbon cycle processes can influence the large-scale climate of the model. Lifting this restriction whilst maintaining a realistic climate simulation, and assessing the climate and sensitivities of this fully interactive carbon cycle version of FAMOUS is beyond the scope of this paper, and will be addressed in a forthcoming publication.

Future work with FAMOUS aims to incorporate further ocean biogeochemical processes related to long timescale responses of the ocean carbon cycle (such as weathering); analogous to the GENIE Earth system model (e.g. Ridgwell and Hargreaves, 2007). This will enable more realistic multi-centennial climate simulations to be carried out with a view to aiding a better understanding of ocean acidification under climate change, for example. Work is also underway to improve the coupling between FAMOUS and the Glimmer icesheet model by including a detailed representation of sub-gridscale orography and snowpack behaviour.

Acknowledgement. JHTW and PJV were supported by funding from Statoil ASA, Norway. JHTW and PJV thank T. L. Leith of Statoil ASA for extensive discussions throughout this work.

References

- Booth, B. B. B., Jones, C. D., Collins, M., Totterdell, I. J., Cox, P. M., Sitch, S., Huntingford, C., Betts, R. A., Harris, G. R., and Lloyd, J.: High sensitivity of future global warming to land carbon cycle processes, *Environ. Res. Lett.*, 7, 024002, doi:10.1088/1748-9326/7/2/024002, 2012.
- Boyd, P. W., Watson, A. J., Law, C. S., Abraham, E. R., Trull, T., Murdoch, R., Bakker, D. C. E., Bowie, A. R., Buesseler, K. O., Chang, H., Charette, M., Croot, P., Downing, K., Frew, R., Gall, M., Hadfield, M., Hall, J., Harvey, M., Jameson, G., LaRoche, J., Liddicoat, M., Ling, R., Maldonado, M. T., McKay, R. M., Nodder, S., Pickmere, S., Pridmore, R., Rintoul, S., Safi, K., Sutton, P., Strzepek, R., Tanneberger, K., Turner, S., Waite A., and Zeldis, J.: A mesoscale phytoplankton bloom in the polar Southern Ocean stimulated by iron fertilisation, *Nature*, 407, 695–702, 2000.
- Cox, P. M.: Description of the “TRIFFID” dynamic global vegetation model, Hadley Centre Technical Note 24, 17 pp., 2001.
- Cox, P. M., Huntingford, C., and Harding, R. J.: A canopy conductance and photosynthesis model for use in a GCM land surface scheme, *J. Hydrol.*, 212, 79–94, 1998.
- Cox, P. M., Betts, R. A., Bunton, C. B., Essery, R. L. H., Rowntree, P. R., and Smith, J.: The impact of new land surface physics on the GCM sensitivity of climate and climate sensitivity, *Clim. Dyn.*, 15, 183–203, 1999.
- Cox, P. M., Betts, R. A., Jones, C. D., Spall, S. A., and Totterdell, I. J.: Acceleration of global warming due to carbon cycle feedbacks in a coupled climate model, *Nature*, 408, 184–187, 2000.
- Doney, S. C., Lindsay, K., Caldeira, K., Campin, J.-M., Drange, H., Dutay, J.-C., Follows, M., Gao, Y., Gnanadesikan, A., Gruber, N., Ishida, A., Joos, F., Madec, G., Maier-Reimer, E., Marshall, J. C., Matear, R. J., Monfray, P., Mouchet, A., Najjar, R., Orr, J. C., Plattner, G.-K., Sarmiento, J., Schlitzer, R., Slater, R., Totterdell, I. J., Weirig, M.-F., Yamanaka, Y., and Yool, A.: Evaluating global ocean carbon models: The importance of realistic physics. *Global Biogeochem. Cy.*, 18, GB3017, doi:10.1029/2003GB002150, 2004.
- Eppley, R. W.: Temperature and phytoplankton growth in the sea, *Fish. Bull.*, 70, 1063–1085, 1972.
- Essery, R. L. H., Best, M. J., Betts, R. A., and Cox, P. M.: Explicit representation of subgrid heterogeneity in a GCM land surface scheme, *J. Hydrometeorol.*, 4, 530–543, 2003.

GMDD

5, 3089–3129, 2012

Optimising the FAMOUS climate model: inclusion of global carbon cycling

J. H. T. Williams et al.

[Title Page](#)

[Abstract](#)

[Introduction](#)

[Conclusions](#)

[References](#)

[Tables](#)

[Figures](#)

[⏪](#)

[⏩](#)

[◀](#)

[▶](#)

[Back](#)

[Close](#)

[Full Screen / Esc](#)

[Printer-friendly Version](#)

[Interactive Discussion](#)

Optimising the FAMOUS climate model: inclusion of global carbon cycling

J. H. T. Williams et al.

[Title Page](#)

[Abstract](#)

[Introduction](#)

[Conclusions](#)

[References](#)

[Tables](#)

[Figures](#)



[Back](#)

[Close](#)

[Full Screen / Esc](#)

[Printer-friendly Version](#)

[Interactive Discussion](#)



Garcia, H. E., Locarnini, R. A., Boyer, T. P., and Antonov, J. I.: World Ocean Atlas 2005, Vol. 4: Nutrients (phosphate, nitrate, silicate), edited by: Levitus, S., NOAA Atlas NESDIS 64, US Government Printing Office, Washington, D. C., 396 pp., 2006.

Gordon, C., Cooper, C., Senior, C. A., Banks, H., Gregory, J. M., Johns T. C., Mitchell, J. F. B., and Wood, R. A.: The simulation of SST, sea ice extents and ocean heat transports in a version of the Hadley Centre coupled model without flux adjustments, *Clim. Dyn.*, 16, 147–168, 2000.

Gregoire, L. J., Valdes, P. J., Payne, A. J., and Kahana, R.: Optimal tuning of a GCM using modern and glacial constraints, *Clim. Dyn.*, 37, 705–719, doi:10.1007/s00382-010-0934-8, 2010.

Jones, C., Gregory, J., Thorpe, R., Cox, P., Murphy, J., Sexton, D., and Valdes, P.: Systematic optimisation and climate simulations of FAMOUS, a fast version of HadCM3, *Clim. Dyn.*, 25, 189–204, 2005.

Law, B. E., Arkebauer, T., Campbell, J. L., Chen, J., Sun, O., Schwartz, M., van Ingen, C., and Verma, S.: Terrestrial carbon observations: protocols for vegetation sampling and data submission, Food and Agricultural Organisation of the United Nations, Rome, 87 pp., 2008.

Loveland, T. R., Reed, B. C., Brown, J. F., Ohlen, D. O., Zhu, Z., Yang, L., and Merchant, J. W.: Development of a global land cover characteristics database and IGBP DISCover from 1 km AVHRR data, *Int. J. Remote Sens.*, 21, 1303–1330, 2000.

Maslin, M., Malhi, Y., Phillips, O., and Cowling, C.: New views on an old forest: assessing the longevity, resilience and future of the Amazon rainforest, *T. I. Brit. Geogr.*, 30, 477–499, 2005.

Murphy, J. M., Sexton, D. M. H., Barnett, D., N., Jones, G. S., Webb, M. J., Collins, M., and Stainforth, D. A.: Quantification of modelling uncertainties in a large ensemble of climate change simulation, *Nature*, 430, 768–772, 2004.

Palmer, J. R. and Totterdell, I. J.: Production and export in a global ocean ecosystem model, *Deep-Sea Res. Pt. I*, 48, 1169–1198, 2001.

Pope, V. D., Gallani, M. L., Rowntree P. R., and Stratton, R. A.: The impact of new physical parametrizations in the Hadley Centre climate model – HadAM3, *Clim. Dyn.*, 16, 123–146, 2000.

Rayner, N. A., Parker, D. E., Horton, E. B., Folland, C. K., Alexander, L. V., Rowell, D. P., Kent, E. C., and Kaplan, A.: Global analyses of sea surface temperature, sea ice, and

Optimising the FAMOUS climate model: inclusion of global carbon cycling

J. H. T. Williams et al.

[Title Page](#)

[Abstract](#)

[Introduction](#)

[Conclusions](#)

[References](#)

[Tables](#)

[Figures](#)

[⏪](#)

[⏩](#)

[◀](#)

[▶](#)

[Back](#)

[Close](#)

[Full Screen / Esc](#)

[Printer-friendly Version](#)

[Interactive Discussion](#)



night marine air temperature since the late nineteenth century, *J. Geophys. Res.*, 108, 4407 doi:10.1029/2002JD002670, 2003.

Redfield, A. C.: The biological control of chemical factors in the environment, *Am. Sci.*, 46, 205–221, 1958.

5 Ridgwell, A. and Hargreaves, J. C.: Regulation of atmospheric CO₂ by deep-sea sediments in an Earth system model, *Global Biogeochem. Cy.*, 21, GB2008, doi:10.1029/2006GB002764, 2007.

Scott, V., Kettle, H., and Merchant, C., J.: Sensitivity analysis of an ocean carbon cycle model in the North Atlantic: An investigation of parameters affecting the air-sea CO₂ flux, primary production and export of detritus, *Ocean Sci.*, 7, 405–419, 2011, <http://www.ocean-sci.net/7/405/2011/>.

10 Smith, R. S., Gregory, J. M., and Osprey, A.: A description of the FAMOUS (version XDBUA) climate model and control run. *Geosci. Model Dev.*, 1, 53–68, doi:10.5194/gmd-1-53-2008, 2008.

15 Smith, R. S.: The FAMOUS climate model (versions XFXWB and XFHCC): description update to version XDBUA, *Geosci. Model Dev.*, 5, 269–276, doi:10.5194/gmd-5-269-2012, 2012.

Uppala, S. M., Kållberg, P. W., Simmons, A. J., Andrae, U., da Costa Bechtold, V., Fiorino, M., Gibson, J. K., Haseler, J., Hernandez, A., Kelly, G. A., Li, X., Onogi, K., Saarinen, S., Sokka, N., Allan, R. P., Andersson, E., Arpe, K., Balmaseda, M. A., Beljaars, A. C. M., Van de Berg, L., Bidlot, J., Bormann, N., Caires, S., Chevallier, F., Dethof, A., Dragosavac, M., Fisher, M., Fuentes, M., Hagemann, S., Hólm, E., Hoskins, B. J., Isaksen, L., Janssen, P. A. E. M., Jenne, R., McNally, A. P., Mahfouf, J.-F., Morcrette, J.-J., Rayner, N. A., Saunders, R. W., Simon, P., Sterl, A., Trenberth, K. E., Untch, A., Vasiljevic, D., Viterbo, P., and Woollen, J.: The ERA-40 re-analysis, *Q. J. R. Meteorolog. Soc.*, 131, 2961–3012, doi:10.1256/qj.04.176, 2005.

25 Watterson, I. G.: Non-dimensional measures of climate model performance, *Int. J. Climatol.*, 16, 379–391, 1996.

Werth, D., and Avissar, R.: The local and global effects of Amazon deforestation, *J. Geophys. Res.*, 107, 8087, doi:10.1029/2001JD000717, 2002.

30 Xie, P., and Arkin, P. A.: Global precipitation: a 17-year monthly analysis based on gauge observations, satellite estimates, and numerical model outputs, *B. Am. Meteorol. Soc.*, 78, 2539–2558, 1997.

Optimising the FAMOUS climate model: inclusion of global carbon cycling

J. H. T. Williams et al.

Table 1. List of parameters used in the land surface carbon cycle perturbed physics ensemble. The values of the minimum leaf area index (LAI) for C3, C4 and shrubs are not varied in this work and hence only one value is given. The three different parameters used are (1) the minimum value used in the Latin hypercube sampling scheme (2) the “standard” value used in the simulation framework before parameter perturbation and (3) the maximum value. Note that the ranges used in this work are the same as in Booth et al. (2012). The additional R_{grow} parameter in this work is varied by 50 % either side of its standard value.

	BT	NT	C3	C4	Shrub
N_{Lo}	0.018, 0.03, 0.1	0.024, 0.03, 0.082	0.028, 0.06, 0.152	0.018, 0.03, 0.188	0.018, 0.03, 0.096
f_0	0.7, 0.875, 0.95	0.7, 0.875, 0.95	0.7, 0.9, 0.95	0.65, 0.8, 0.8	0.7, 0.9, 0.95
LAI_{min}	1, 3, 4	1, 3, 4	1	1	1
Q_{10}	1.5, 2, 3.5	1.5, 2, 3.5	1.5, 2, 3.5	1.5, 2, 3.5	1.5, 2, 3.5
α	0, 0.5, 1	0, 0.5, 1	0, 0.5, 1	0, 0.5, 1	0, 0.5, 1
T_{upp}	31, 36, 41	$T_{\text{upp, BT}} - 5.0$	$T_{\text{upp, BT}}$	$T_{\text{upp, BT}} + 9.0$	$T_{\text{upp, BT}}$
R_{grow}	0.125, 0.25, 0.375	0.125, 0.25, 0.375	0.125, 0.25, 0.375	0.125, 0.25, 0.375	0.125, 0.25, 0.375

[Title Page](#)
[Abstract](#)
[Introduction](#)
[Conclusions](#)
[References](#)
[Tables](#)
[Figures](#)
[Back](#)
[Close](#)
[Full Screen / Esc](#)
[Printer-friendly Version](#)
[Interactive Discussion](#)

Optimising the FAMOUS climate model: inclusion of global carbon cycling

J. H. T. Williams et al.

[Title Page](#)

[Abstract](#)

[Introduction](#)

[Conclusions](#)

[References](#)

[Tables](#)

[Figures](#)



[Back](#)

[Close](#)

[Full Screen / Esc](#)

[Printer-friendly Version](#)

[Interactive Discussion](#)

Table 2. Control structural parameters in the HadOCC ecosystem model.

Model parameter name	Control parameter value (units)	Physical interpretation	Free parameter index (see text)
c2n_p	6.625	C : N ratio for phytoplankton	1
c2n_z	5.625	C : N ratio for zooplankton	1
c2n_d	7.5	C : N ratio for detritus	1
psmax	0.6	Maximum rate of photosynthesis	2
alpha	0.02 ((W m ⁻²) ⁻¹ day ⁻¹)	Initial slope of photosynthesis – irradiance curve	2
Q10H	1.0	Increase in phytoplankton growth rate for a 10 degree temperature increase	2
mort_sat	0.1 (mMol m ⁻³)	Half-saturation constant for phytoplankton mortality	2
resp_rate	0.02 (day ⁻¹)	Rate of phytoplankton respiration in fraction of biomass lost per day	2
pmort_max	0.05 (day ⁻¹ (mMol m ⁻³) ⁻¹)	Maximum phytoplankton mortality (expressed as biomass fraction lost per day)	2
graze_max	1.0 (day ⁻¹)	Maximum specific rate of zooplankton grazing	3
graze_sat	0.75 (mMol m ⁻³)	Half-saturation constant for zooplankton grazing	3
graze_threshold	0.1 (mMol m ⁻³ day ⁻¹)	Threshold for zooplankton grazing function	3
beta_p	0.7	Assimilation efficiency of zooplankton feeding of phytoplankton	3
beta_dt	0.5	Assimilation efficiency of zooplankton feeding on detritus	3
z_mort_1	0.02 (day ⁻¹)	Linear zooplankton mortality	3
z_mort_2	0.3 (day ⁻¹ (mMol m ⁻³) ⁻¹)	Quadratic zooplankton mortality	3
remin_rate_shallow	0.1 (day ⁻¹)	Remineralisation rate, levels 1 to 8	4
remin_rate_deep	0.02 (day ⁻¹)	Remineralisation rate, levels 9 to 20	4
sink_rate_dt	10.0 (m day ⁻¹)	Sinking rate for detritus	4
rain_ratio	0.007	Carbon export as calcite, as a proportion of primary production	5

Optimising the FAMOUS climate model: inclusion of global carbon cycling

J. H. T. Williams et al.

[Title Page](#)

[Abstract](#)

[Introduction](#)

[Conclusions](#)

[References](#)

[Tables](#)

[Figures](#)



[Back](#)

[Close](#)

[Full Screen / Esc](#)

[Printer-friendly Version](#)

[Interactive Discussion](#)

Table 3. Parameter values for the highest scoring ocean carbon cycle ensemble member and their relationship to the respective control value.

Parameter	Values from highest scoring ensemble member	Percentage of control value
c2n_p	6.559	99.0 %
c2n_z	5.569	
c2n_d	7.426	
psmax	0.8417	
alpha	0.02806	140.3 %
Q10H	1.403	
mort_sat	0.1403	
resp_rate	0.02806	
pmort_max	0.07014	
graze_max	1.297	129.7 %
graze_sat	0.9729	
graze_threshold	0.1297	
beta_p	0.908	
beta_dt	0.6486	
z_mort_1	0.02594	
z_mort_2	0.3891	
remin_rate_shallow	0.06488	64.9 %
remin_rate_deep	0.01298	
sink_rate_dt	6.488	
rain_ratio	0.009729	139.0 %

Optimising the FAMOUS climate model: inclusion of global carbon cycling

J. H. T. Williams et al.

[Title Page](#)

[Abstract](#)

[Introduction](#)

[Conclusions](#)

[References](#)

[Tables](#)

[Figures](#)



[Back](#)

[Close](#)

[Full Screen / Esc](#)

[Printer-friendly Version](#)

[Interactive Discussion](#)

Table 4. Regional and seasonal AMS values for different members of the FAMOUS model hierarchy. These are calculated for 1.5 m air temperature with respect to HadCM3. Generation numbers are given in brackets.

		ADTAN (1)	XDBUA (2)	XFHCC (3)	XFHCU (4a)	XFHCS (4b)
45–90° N	DJF	0.60	0.70	0.79	0.82	0.76
	JJA	0.79	0.76	0.84	0.77	0.68
	Annual	0.66	0.77	0.85	0.84	0.76
Global	DJF	0.85	0.86	0.88	0.87	0.87
	JJA	0.90	0.88	0.88	0.88	0.88
	Annual	0.89	0.89	0.89	0.89	0.89

Optimising the FAMOUS climate model: inclusion of global carbon cycling

J. H. T. Williams et al.

[Title Page](#)

[Abstract](#)

[Introduction](#)

[Conclusions](#)

[References](#)

[Tables](#)

[Figures](#)



[Back](#)

[Close](#)

[Full Screen / Esc](#)

[Printer-friendly Version](#)

[Interactive Discussion](#)

Table 5. Ozone concentrations in kg kg^{-1} around the tropopause for the different generations of FAMOUS.

Level	1st generation	2nd and 3rd generation	4th generation
Top layer	–	1.5×10^{-6}	6.0×10^{-6}
Above tropopause	1.5×10^{-6}	1.0×10^{-6}	2.0×10^{-6}
At tropopause	2.0×10^{-7}	2.0×10^{-7}	1.0×10^{-7}
Below tropopause	2.0×10^{-8}	2.0×10^{-8}	2.0×10^{-8}

Optimising the FAMOUS climate model: inclusion of global carbon cycling

J. H. T. Williams et al.

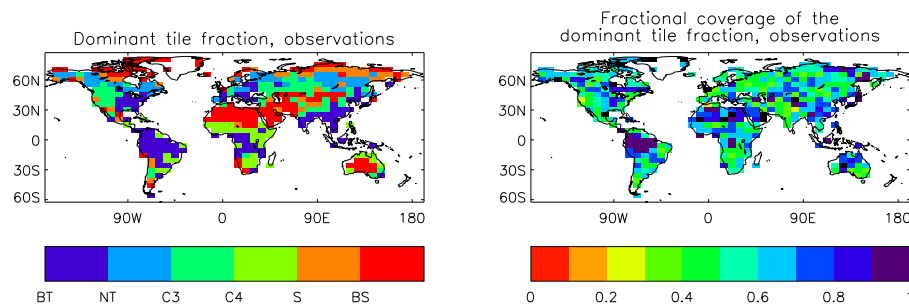


Fig. 1. The left-hand figure shows the observed dominant plant functional type for the present day (Loveland et al., 2000) and the right-hand figure shows the fractional coverage of the dominant type. BT (broadleaf tree), NT (needleleaf tree), C3 and C4 vegetation and S (shrubs) and BS (bare soil).

[Title Page](#)[Abstract](#)[Introduction](#)[Conclusions](#)[References](#)[Tables](#)[Figures](#)[⏪](#)[⏩](#)[◀](#)[▶](#)[Back](#)[Close](#)[Full Screen / Esc](#)[Printer-friendly Version](#)[Interactive Discussion](#)

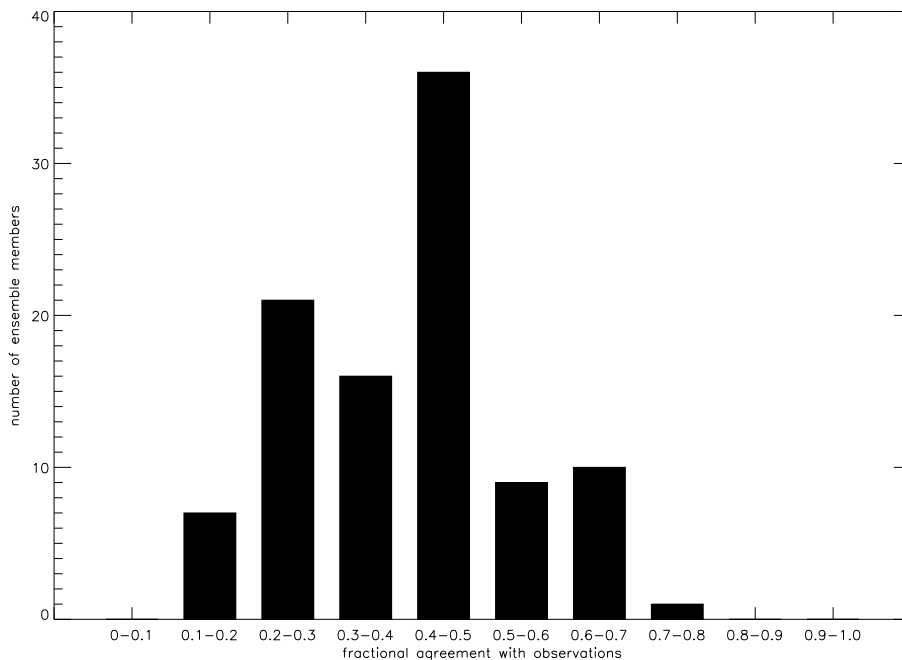


Fig. 2. Histogram of the fractional agreement between the 100 ensemble members and the observations over the Amazon region for all PFTs. Here, “fractional agreement”, gives the fraction of the 28 grid Amazonian grid boxes which are assigned the same PFT in the ensemble members and in observations.

Optimising the FAMOUS climate model: inclusion of global carbon cycling

J. H. T. Williams et al.

[Title Page](#)

[Abstract](#) [Introduction](#)

[Conclusions](#) [References](#)

[Tables](#) [Figures](#)

[⏪](#) [⏩](#)

[◀](#) [▶](#)

[Back](#) [Close](#)

[Full Screen / Esc](#)

[Printer-friendly Version](#)

[Interactive Discussion](#)



Optimising the FAMOUS climate model: inclusion of global carbon cycling

J. H. T. Williams et al.

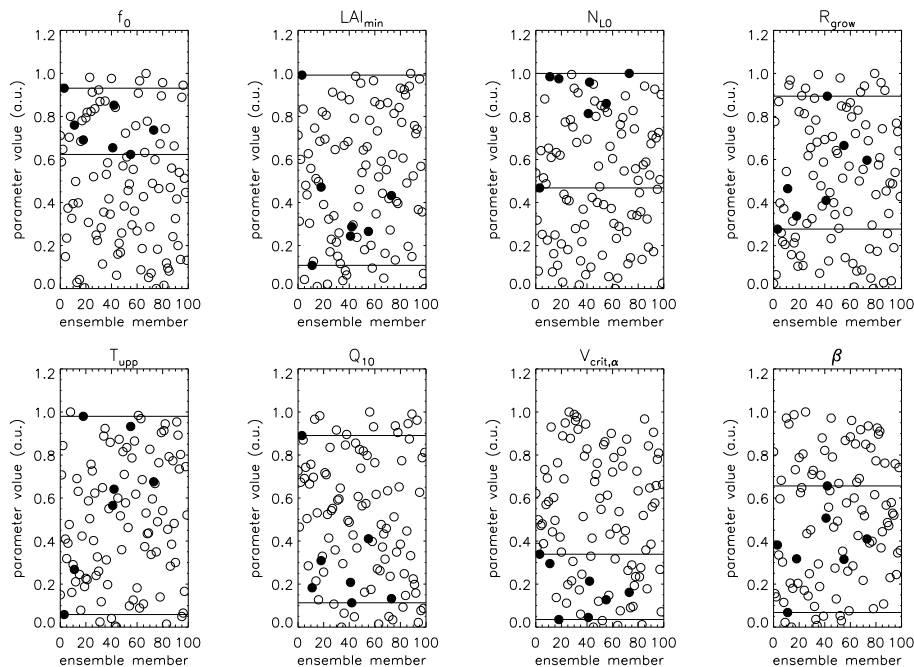


Fig. 3. The sensitivity of the 100 ensemble members to individual parameters. The $\alpha 7$ simulations are shown with filled symbols and the horizontal lines represent the minimum and maximum values of each parameter covered by them.

Title Page

Abstract

Introduction

Conclusions

References

Tables

Figures

⏪

⏩

◀

▶

Back

Close

Full Screen / Esc

Printer-friendly Version

Interactive Discussion

Optimising the FAMOUS climate model: inclusion of global carbon cycling

J. H. T. Williams et al.

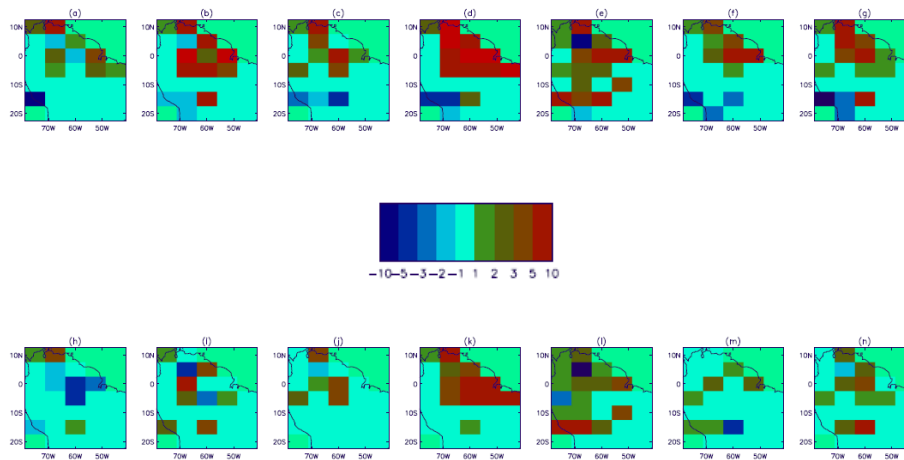


Fig. 4. Difference between the combined-PFT LAI of the mid-Holocene and $\alpha 7$ runs (a–g) and the equivalent residual plots for the LGM and $\alpha 7$ runs (h–n).

Title Page

Abstract

Introduction

Conclusions

References

Tables

Figures



Back

Close

Full Screen / Esc

Printer-friendly Version

Interactive Discussion

Optimising the FAMOUS climate model: inclusion of global carbon cycling

J. H. T. Williams et al.

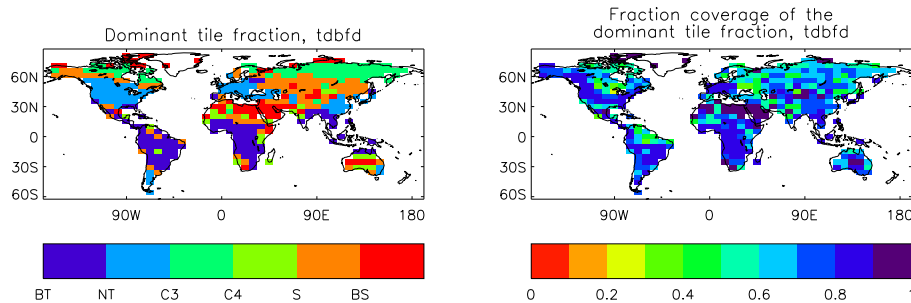


Fig. 5. The left-hand figure shows the simulated dominant plant functional type for the best performing land surface ensemble member and the right-hand figure shows the fractional coverage of the dominant type.

[Title Page](#)[Abstract](#)[Introduction](#)[Conclusions](#)[References](#)[Tables](#)[Figures](#)[⏪](#)[⏩](#)[◀](#)[▶](#)[Back](#)[Close](#)[Full Screen / Esc](#)[Printer-friendly Version](#)[Interactive Discussion](#)

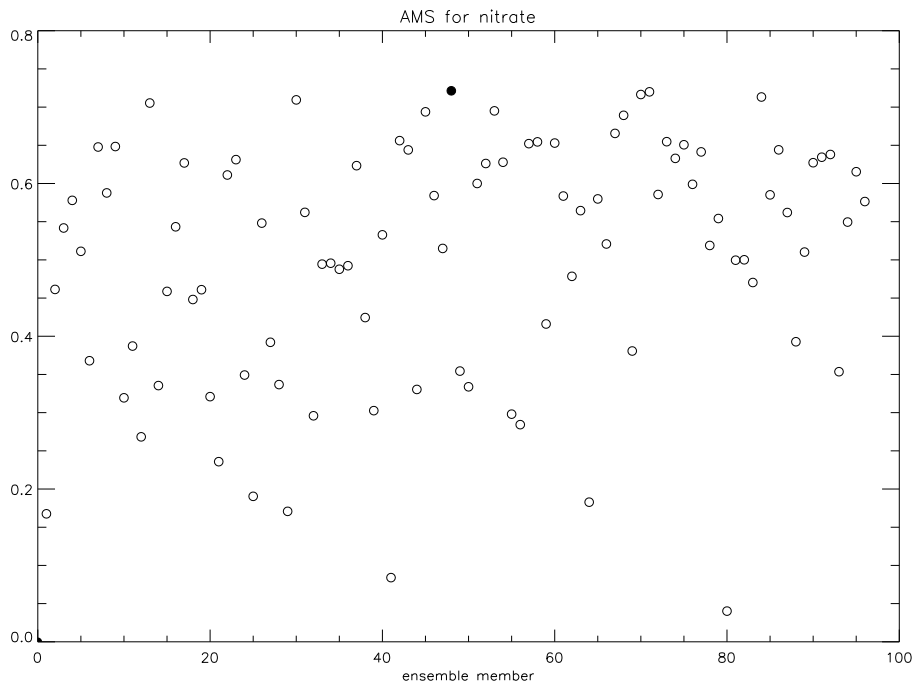


Fig. 6. The AMS for the ocean carbon cycle ensemble’s nitrate concentration when compared against World Ocean Atlas data. The ensemble member giving rise to the highest AMS is marked with a filled circle.

Optimising the FAMOUS climate model: inclusion of global carbon cycling

J. H. T. Williams et al.

[Title Page](#)

[Abstract](#)

[Introduction](#)

[Conclusions](#)

[References](#)

[Tables](#)

[Figures](#)



[Back](#)

[Close](#)

[Full Screen / Esc](#)

[Printer-friendly Version](#)

[Interactive Discussion](#)



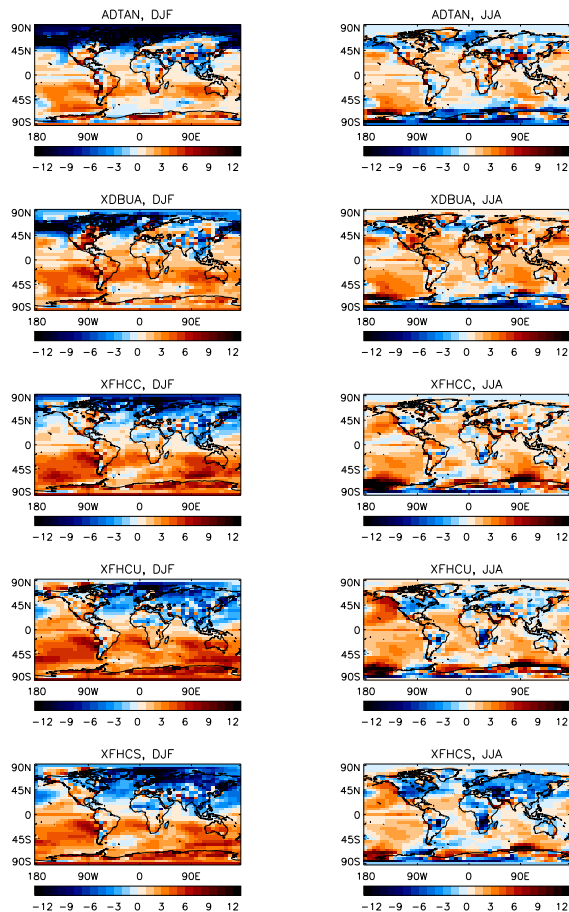


Fig. 7. Air temperature at 1.5 m with respect to HadCM3 for progressively more modern versions of FAMOUS (most recent at the bottom of the figure) for DJF (left) and JJA (right).

Optimising the FAMOUS climate model: inclusion of global carbon cycling

J. H. T. Williams et al.

[Title Page](#)

[Abstract](#)

[Introduction](#)

[Conclusions](#)

[References](#)

[Tables](#)

[Figures](#)

⏪

⏩

◀

▶

[Back](#)

[Close](#)

[Full Screen / Esc](#)

[Printer-friendly Version](#)

[Interactive Discussion](#)



Optimising the FAMOUS climate model: inclusion of global carbon cycling

J. H. T. Williams et al.

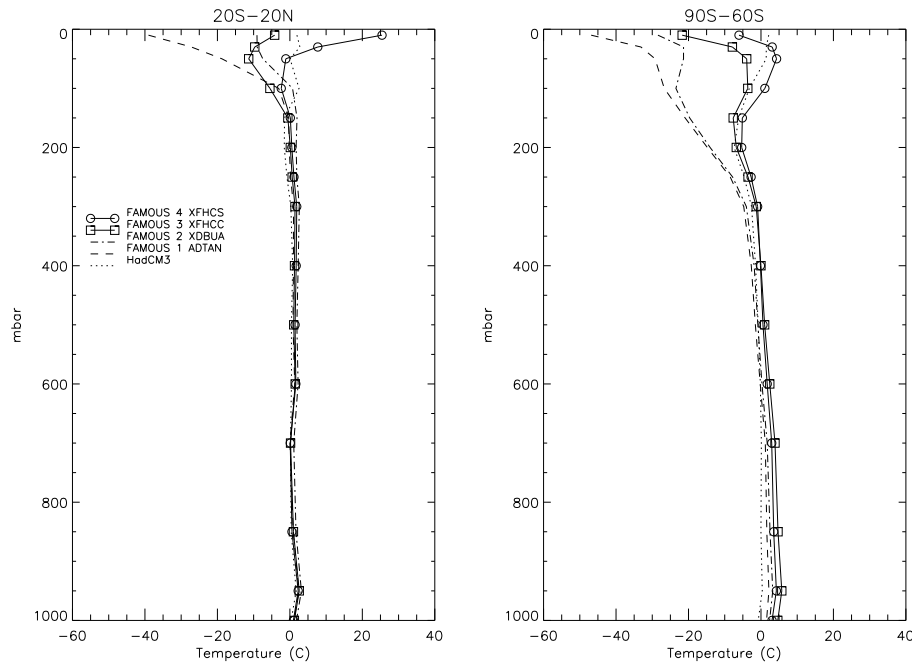


Fig. 8. Mean temperature profiles for 20° S–20° N (left) and 90° S–60° S (right) for HadCM3 (dotted line), generation 1 FAMOUS, ADTAN (dashed line), generation 2, XDBUA (dotted-dashed line), generation 3, XFHCc (squares) and generation 4b, XFHCs (circles). The generation 4a model, XFHCu is not shown since its temperature profile is virtually indistinguishable from the generation 4b version, especially in the stratosphere.

[Title Page](#)
[Abstract](#)
[Introduction](#)
[Conclusions](#)
[References](#)
[Tables](#)
[Figures](#)
[⏪](#)
[⏩](#)
[◀](#)
[▶](#)
[Back](#)
[Close](#)
[Full Screen / Esc](#)
[Printer-friendly Version](#)
[Interactive Discussion](#)

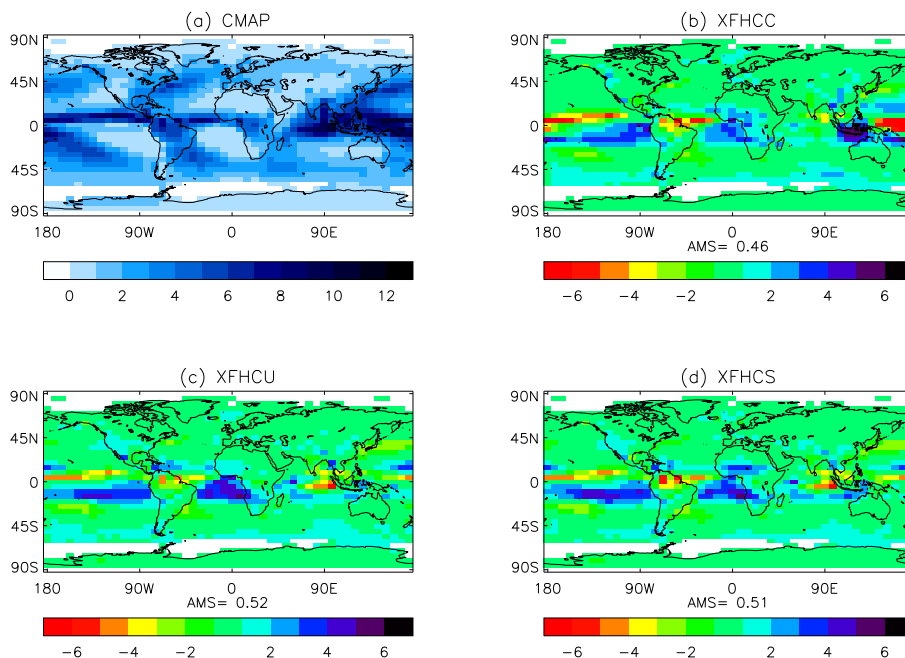


Fig. 9. Annual mean total precipitation rate in mm per day for **(a)** the CMAP climatology (Xie and Arkin, 1997) and the difference between the simulated total precipitation and CMAP for **(b)** the generation 3 model XFHCC, **(c)** the generation 4a model XFHCU and **(d)** the generation 4b model XFHCS. Missing data areas are set to white and the AMS scores for the 3 model generations are given in the subtitles to **(b)**, **(c)** and **(d)**.

Title Page

Abstract

Introduction

Conclusions

References

Tables

Figures

⏪

⏩

◀

▶

Back

Close

Full Screen / Esc

Printer-friendly Version

Interactive Discussion

Optimising the FAMOUS climate model: inclusion of global carbon cycling

J. H. T. Williams et al.

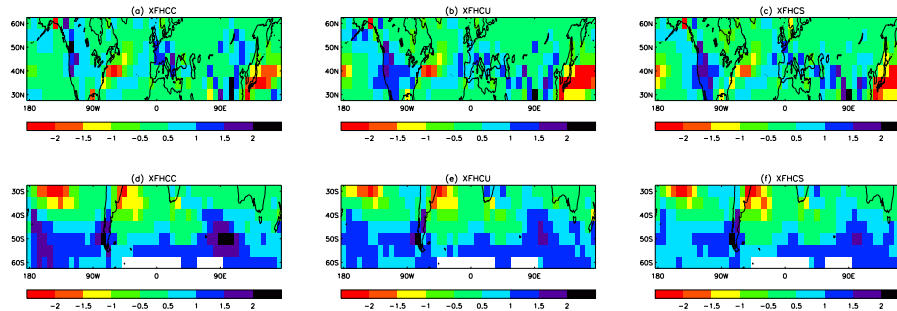


Fig. 10. Difference between simulated and observed precipitation in the northern (**a–c**) and southern (**d–f**) mid-latitudes as shown globally in Fig. 9. Note the different contour intervals compared to Fig. 9.

[Title Page](#)[Abstract](#)[Introduction](#)[Conclusions](#)[References](#)[Tables](#)[Figures](#)[⏪](#)[⏩](#)[◀](#)[▶](#)[Back](#)[Close](#)[Full Screen / Esc](#)[Printer-friendly Version](#)[Interactive Discussion](#)

Optimising the FAMOUS climate model: inclusion of global carbon cycling

J. H. T. Williams et al.

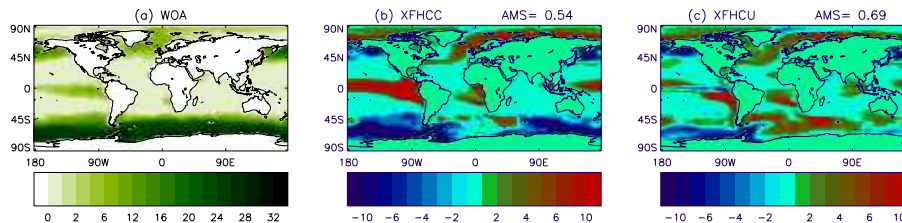


Fig. 11. Annual mean nitrate concentration in mmol per m^{-3} at 5 m for **(a)** World Ocean Atlas observations (Garcia et al., 2006) and the difference between the simulated and observed values for **(b)** the generation 3 model XFHCC, **(c)** the generation 4a model XFHCU. The AMS scores for simulations are given above **(b)** and **(c)**.

Title Page

Abstract

Introduction

Conclusions

References

Tables

Figures

⏪

⏩

◀

▶

Back

Close

Full Screen / Esc

Printer-friendly Version

Interactive Discussion